

# Small but large: Single organic molecules as hybrid platforms for quantum technologies

Burak Gurlek<sup>1,\*</sup> and Daqing Wang<sup>2,†</sup>

<sup>1</sup>*Max Planck Institute for the Structure and Dynamics of Matter,  
Luruper Chaussee 149, 22761 Hamburg, Germany*

<sup>2</sup>*Institute of Applied Physics, University of Bonn, Wegelerstr. 8, 53115 Bonn, Germany*

Single organic molecules embedded in solid-state matrices exhibit remarkable optical properties, making them competitive candidates for single-photon sources and quantum nonlinear optical elements. However, the lack of long-lived internal states imposes significant constraints on their application in the broader field of quantum technologies. In this article, we reexamine the single-molecule host-guest system from first principles, elaborate on the rich internal states this system encompasses and put forward strategies to harness them for applications in quantum memory, spin-photon interface, spin register, and optomechanics. Further, we discuss the potential of leveraging the vast chemical space of molecules, and highlight the challenges and opportunities for molecular systems along these directions.

## I. INTRODUCTION

Since the first detection of a single pentacene molecule in *para*-terphenyl crystal by Moerner *et al.* [1] and Orrit *et al.* [2], the favorable optical properties of polycyclic aromatic hydrocarbon (PAH) molecules have enabled many pioneering advancements in quantum optics [3, 4]. Their preeminent properties of single photon emission, such as the Fourier-limited linewidth, high quantum efficiency, and high photostability make them excellent sources of indistinguishable photons [5–7]. A single molecule can function as an optical nonlinear medium operating in the quantum regime, owing to the anharmonicity of its electronic excited states. This has been utilized to demonstrate a single-molecule optical transistor [8] and frequency mixing between two optical beams [9, 10]. Furthermore, the frequency of molecular photons can be tuned by the Stark effect [11, 12], exciting with a strong pump laser [13] or external strain [14–16]. The fine control over the emission frequency facilitated the interfacing of remote molecules through single photons [17, 18]. Moreover, PAH molecules are compatible with photonic structures such as dielectric [19, 20] and plasmonic antennas [21], optical waveguides [22–26] and on-chip resonators [27]. Recent demonstrations have shown the strong coupling of a single molecule to a Fabry-Pérot microcavity [10, 18]. Having frequency tunability and controllable doping concentration, near-field couplings between two closely spaced molecules via coherent dipole-dipole interactions have also been shown [28–30]. In addition, the narrow-linewidth optical transition makes single molecules ultra-sensitive probes for their local environment, e.g., charge fluctuations [31], and mechanical oscillations [15, 32].

Spectroscopic detection of single PAH molecules relies on their insertion as impurities into a host material,

i.e., forming a host-guest system through van der Waals interactions. With suitable choices of host-guest combinations, such a system can feature two favorable properties. First, the van der Waals interaction allows the electronic excitations of the guest to remain largely localized within its own molecular orbitals, with only weak perturbation from the host. In this regard, the guest’s ground state and lowest electronic excited state facilitate an optical transition, which could feature a nearly lifetime-limited linewidth at liquid helium temperatures, on par with atomic transitions in vacuum [3]. Second, this transition can be approximated as a two-level cycling transition, where population decays to other levels are recycled through interactions with the matrix, e.g., fast vibrational relaxation, allowing measurements using only a single laser beam. It is worth noting that the success of most past achievements in molecular quantum optics builds primarily upon the efficient isolation of such a two-level transition. Beyond this simplified two-level picture, the molecular host-guest system represents a hybrid quantum system, incorporating electronic, nuclear, and spin degrees of freedom [33]. The presence of this multitude of couplings has been considered detrimental, as they introduce incoherent leakage channels.

In this article, we introduce single molecules embedded in a solid-state host as a hybrid quantum system, provide a detailed discussion of its various degrees of freedom, and outline the prospects of harnessing them for applications that have not been realized on molecular systems so far. The article is organized as follows. In section II, we examine the molecular host-guest system from first principles, revisit its wavefunction, energy landscape, and associated transitions. A particular focus will be given to the quantum nature of its vibrational and spin degrees of freedom. In section III, we discuss the potential of using vibrational and spin states for molecular quantum memory, optomechanics, spin-photon interfaces and chemically configurable spin registers. We will further expand the discussion towards exploring the vast chemical space of molecules for quantum applications. Finally, we

\* burak.gurlek@mpsd.mpg.de

† daqing.wang@uni-bonn.de

discuss the theoretical and experimental challenges associated with these approaches in section IV and conclude with section V.

## II. EMERGING INSIGHTS INTO MOLECULAR HOST-GUEST SYSTEMS

Molecules have emerged as engineerable building blocks for future quantum technologies, thanks to their

rich internal structures and the vast diversity offered by the chemical space [3, 34–36]. Figure 1 illustrates the multiple degrees of freedom in the molecular host-guest system and their couplings. While there is also growing interest in exploiting these internal states [37–40], earlier studies have predominantly focused on the electronic degree of freedom [3], leaving other intriguing aspects largely unexplored. To highlight the promise of molecular host-guest systems for future explorations in quantum science, we revisit these “overlooked” internal states, with a focus on their quantum mechanical character and interactions. Drawing inspiration from previous works [41], we perform a first-principle analysis of molecular host-guest systems to explore their quantum mechanical character in detail.

### A. Revisiting the Host-Guest Wavefunction

The wavefunction of a molecular host-guest system can be expressed following the Born-Oppenheimer approximation similar to the case for a single molecule as

$$\Psi \approx \Psi_{\text{el}}(\mathbf{r}, \mathbf{s}; \mathbf{R}, \mathbf{I}) \Psi_{\text{nuc}}(\mathbf{R}, \mathbf{I}), \quad (1)$$

where the terms on the right-hand side represent the many-body electronic wavefunction of  $n_e$  electrons of all host and guest molecules with spatial  $\mathbf{r} = (\mathbf{r}_1, \mathbf{r}_2, \dots, \mathbf{r}_{n_e})$  and spin coordinates  $\mathbf{s} = (\mathbf{s}_1, \mathbf{s}_2, \dots, \mathbf{s}_{n_e})$ , and the many-body nuclear wavefunction of  $n_n$  nuclei of all host and guest molecules with spatial  $\mathbf{R} = (\mathbf{R}_1, \mathbf{R}_2, \dots, \mathbf{R}_{n_n})$  and spin coordinates  $\mathbf{I} = (\mathbf{I}_1, \mathbf{I}_2, \dots, \mathbf{I}_{n_n})$ , respectively. Typically, a large-band-gap host material is chosen such that its lowest electronic excitation is energetically higher than the states of interest in the guest. In this case, the electronic excitation of the guest remains well isolated from the host. It is thus possible to separate the electronic degrees of freedom such that

$$\Psi_{\text{el}} \approx \Psi_{\text{el,guest}}(\mathbf{r}_g, \mathbf{s}_g; \mathbf{R}, \mathbf{I}) \Psi_{\text{el,host}}(\mathbf{r}_h, \mathbf{s}_h; \mathbf{R}, \mathbf{I}), \quad (2)$$

where  $\mathbf{r}_g, \mathbf{s}_g$  ( $\mathbf{r}_h, \mathbf{s}_h$ ) denote the spatial and spin coordinates of the guest (host), respectively. When studying low-lying excitations in the guest, the electronic states of the host are unaffected and can be traced out<sup>1</sup>. Hence, the system’s electronic wavefunction reduces to the spin-orbital state of the guest  $\Psi_{\text{el,guest}}$  (see lower panel of Fig. 1).

Considering the nuclear wavefunction, the interaction between the spin state and the mechanical motion of the nuclei is relatively weak compared to the dominant electrostatic interactions that govern nuclear motion, it is

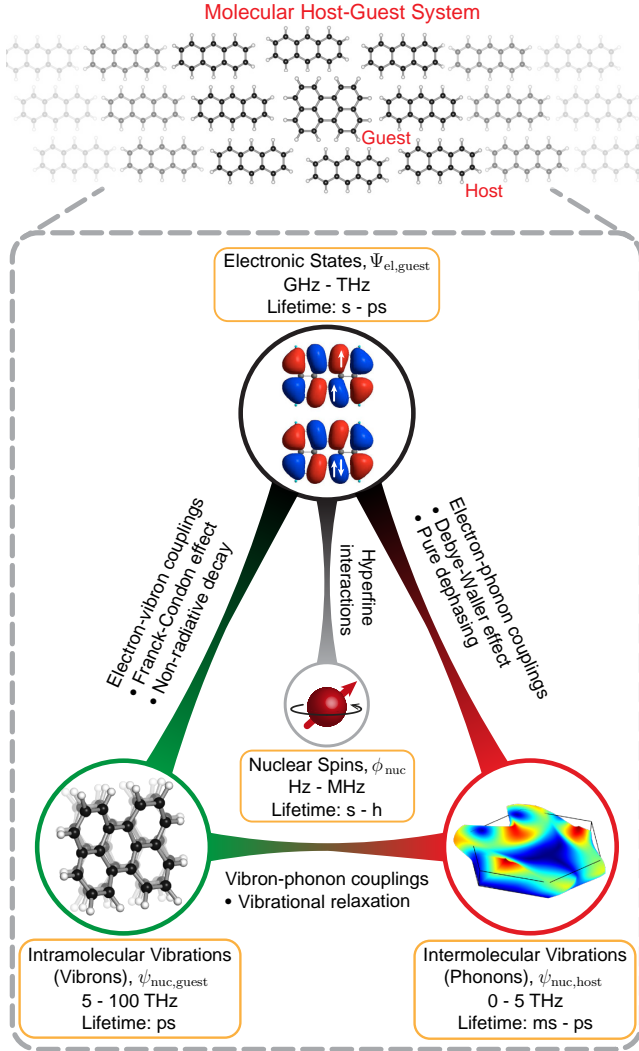


FIG. 1. Upper panel: Illustration of a molecular host-guest system, specifically shown here for anthracene crystal hosting a perylene molecule. Lower Panel: Schematics for the relevant states and their couplings in a molecular host-guest system. The guest’s spin-orbital states (top) interact with its own intramolecular vibrations (bottom left) and intermolecular vibrations of the host crystal (bottom right) via electron-vibron and electron-phonon couplings, respectively. Electronic states are further coupled to nuclear spin degrees of freedom via hyperfine interactions (middle). The vibrational states are coupled to each other via vibron-phonon couplings.

<sup>1</sup> Note that the host’s electronic degrees of freedom plays an important role in determining the geometry of the guest molecule in the solid state.

thus feasible to separate these two degrees of freedom following

$$\Psi_{\text{nuc}}(\mathbf{R}, \mathbf{I}) \approx \psi_{\text{nuc}}(\mathbf{R})\phi_{\text{nuc}}(\mathbf{I}). \quad (3)$$

Moreover, decoupling of the host and guest molecular orbitals allows the decomposition of the nuclear wavefunction into those of the host and the guest. The composite nuclear wavefunction can be expressed in terms of the normal modes of the guest molecule and the host matrix with coordinates  $\mathbf{Q}$  and  $\mathbf{u}$  as [41, 42]

$$\psi_{\text{nuc}}(\mathbf{R}) \approx \psi_{\text{nuc,guest}}(\mathbf{Q})\psi_{\text{nuc,host}}(\mathbf{u}), \quad (4)$$

where  $\psi_{\text{nuc,guest}}(\mathbf{Q})$  and  $\psi_{\text{nuc,host}}(\mathbf{u})$  denote the intramolecular guest and intermolecular host vibrational wavefunctions (see bottom part of Fig. 1). In the remainder of the text, we use the terms *vibron* for the quantized intramolecular normal modes of guest molecule and *phonon* for the quantized intermolecular normal modes of host matrix.

As a result, the wavefunction of the host-guest system can be approximated as

$$\begin{aligned} \Psi \approx & \Psi_{\text{el,guest}}(\mathbf{r}_g, \mathbf{s}_g; \mathbf{R}, \mathbf{I})\psi_{\text{nuc,guest}}(\mathbf{Q}) \\ & \times \psi_{\text{nuc,host}}(\mathbf{u})\phi_{\text{nuc}}(\mathbf{I}), \end{aligned} \quad (5)$$

with their order reflecting the hierarchy of energy scales associated with these states.

Excitations across these various degrees of freedom result in the complex energy level structure depicted in Fig. 2(a). Depending on the total electron spin quantum number  $S$ , the guest's electronic state  $\Psi_{\text{el,guest}}$  can be represented as  $|S_0\rangle, |S_1\rangle, \dots$  for *singlet states* with  $S = 0$ , or  $|T_1\rangle, |T_2\rangle, \dots$  for *triplet states* with  $S = 1$ . The energy levels in Fig. 2(a) can be thus grouped into singlet and triplet manifolds based on  $\Psi_{\text{el,guest}}$ . We focus primarily on three, namely the ground state ( $S_0$ ), lowest-singlet excited state ( $S_1$ ) and lowest-triplet excited state ( $T_1$ ) manifolds, as they play the most important role in molecular quantum optics.

Each manifold encompasses a range of vibron and phonon states, which can be written as  $|\nu_v, \nu_p\rangle$  in the Fock state representation of the vibron and phonon wavefunctions. Here,  $|\nu_v\rangle = \prod_i |\nu_v^{(i)}\rangle$  and  $|\nu_p\rangle = \prod_i |\nu_p^{(i)}\rangle$  denotes the occupation of vibron and phonon modes with vibrational quantum numbers  $\nu_v^{(i)}$  and  $\nu_p^{(i)}$  for the  $i^{\text{th}}$  vibron and phonon modes, respectively. In addition, the many-body nuclear spin states can be expressed as  $\phi_{\text{nuc}}(\mathbf{I}) = \sum_{\{m_{I_i}\}} C_{\{m_{I_i}\}} \otimes_{i=1}^{n_n} |I_i, m_{I_i}\rangle$ , which denotes a linear superposition of basis states formed by the tensor products of uncoupled spin states  $|I_i, m_{I_i}\rangle$  from  $n_n$  nuclei, with the corresponding coefficients  $C_{\{m_{I_i}\}} = C_{m_{I_1}, m_{I_2}, \dots, m_{I_{n_n}}}$ . Here,  $I_i$  and  $m_{I_i}$  denote the spin quantum numbers of the  $i^{\text{th}}$  nucleus. As a result, the wavefunction stemming from Eq. (1) can be represented as

$$\Psi \approx |S(T)_j; \nu_v, \nu_p; I_i, m_{I_i}\rangle, \quad (6)$$

where  $j$  is the integer index of the spin-orbital state. In the following discussion of electronic and vibronic transitions, we will first omit the nuclear spin states, as they primarily manifest through hyperfine interactions with electron spins and are relevant only when probing the triplet manifold, such as in optically detected magnetic resonance experiments. We will revisit these states in the discussion of spin states.

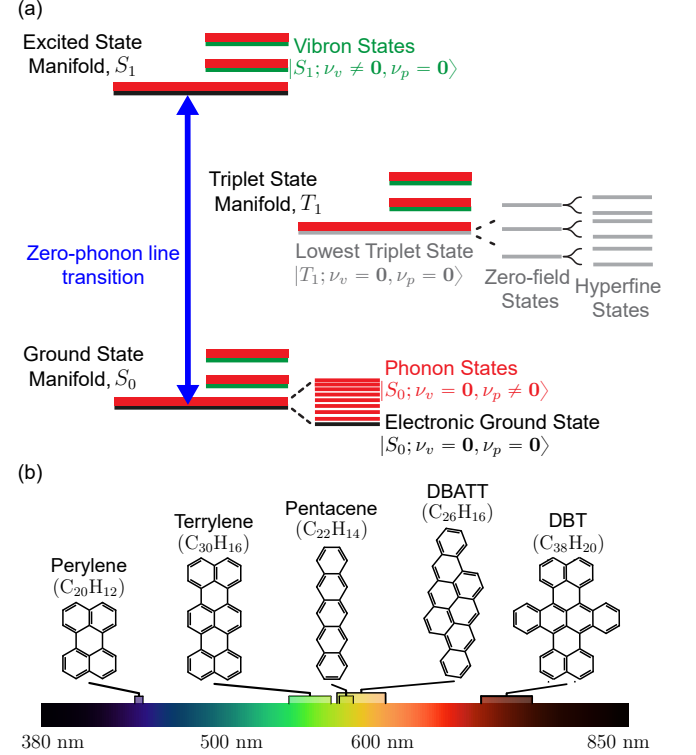


FIG. 2. (a) The energy levels of a single molecule embedded in a matrix. The state  $|S_{0(1)}; \nu_v, \nu_p\rangle$  belongs to the ground (excited) state manifold and has vibrational occupations in the intramolecular  $|\nu_v\rangle = \prod_i |\nu_v^{(i)}\rangle$  and intermolecular vibrational modes  $|\nu_p\rangle = \prod_i |\nu_p^{(i)}\rangle$ . The indices  $\nu_{v(p)}^{(i)} = 0, 1, \dots$  denote the vibrational quantum number of the  $i^{\text{th}}$  vibron (phonon) mode. Similarly,  $|T_1; \nu_v, \nu_p\rangle$  represents the states in the triplet state manifold. (b) PAH molecules commonly used in quantum optics experiments and their range of approximated zero-phonon-line wavelengths [43].

### 1. Ground and excited states

The ground state of the system  $|S_0; \nu_v = 0, \nu_p = 0\rangle$  is a singlet state, in which all  $\pi$ -orbitals are filled and all electron spins are paired. The excitation of one electron to a  $\pi^*$  orbital leaves the molecule in the lowest singlet excited state  $|S_1; \nu_v = 0, \nu_p = 0\rangle$ . Alternatively, if this excitation is accompanied by a spin-flip, the molecule reaches the lowest triplet excited state  $|T_1; \nu_v = 0, \nu_p = 0\rangle$ . The energy of  $|T_1; \nu_v = 0, \nu_p = 0\rangle$

is lower than that of  $|S_1; \nu_v = \mathbf{0}, \nu_p = \mathbf{0}\rangle$  by the exchange energy. The transition energies of these two excited states to the ground state lie in the optical frequency domain and range from UV to near-infrared wavelengths, depending on the size and geometry of the molecule. The triplet state  $|T_1; \nu_v = \mathbf{0}, \nu_p = \mathbf{0}\rangle$  consists of three sub-levels, resulting from the anisotropic magnetic dipole-dipole interactions of two unpaired electrons, which remain non-degenerate even in the absence of an external magnetic field [44]. This is called *zero-field splitting* (ZFS). For PAH molecules emitting in the UV to visible range, the ZFS can reach a few gigahertz [45]. Moreover, coupling of the electron spin to nuclear spins in the molecule and the matrix leads to *hyperfine splittings*, which lie in the radio-frequency range.

In addition, each manifold includes vibron states  $|S(T), \nu_v \neq \mathbf{0}, \nu_p = \mathbf{0}\rangle$  corresponding to librational and bond vibrations of the guest molecule, with frequencies that can reach up to 100 THz. The coupling between electronic and intramolecular vibrational states (electron-vibron coupling) gives rise to the well-known Franck-Condon physics, where the displacement of the excited state potential energy surface along a normal-mode coordinate enables transitions between vibronic states in different manifolds. The transition probabilities, i.e., *Franck-Condon factors*, are related to the *Huang-Rhys factor* of each normal mode [46]. For certain PAH molecules, the simple Franck-Condon picture can be further complicated by the Herzberg-Teller effect, where couplings between the electronic and nuclear degrees of freedom are not parametric [47, 48]. Furthermore, non-adiabatic couplings between the electronic and nuclear degrees of freedom result in non-radiative decay from the excited state manifold via electron-vibron couplings [49, 50]. This could lead to non-unity quantum efficiencies of photon emission [20, 51].

Besides, phonon states  $|S(T), \nu_v = \mathbf{0}, \nu_p \neq \mathbf{0}\rangle$  typically fall within the 0 – 5 THz range and lead to the deformation of molecular orbitals. The resulting electron-phonon couplings yield various optical transitions between different manifolds involving vibrons and phonons, similar to the Franck-Condon physics discussed earlier. Depending on the frequency range, these vibrational states exhibit lifetimes in the range of milliseconds to picoseconds due to different vibrational relaxation mechanisms [52].

## 2. Zero-phonon-line transition

Despite the complexity of the energy structure shown in Fig. 2(a), decay to the ground state manifold typically occurs from the lowest singlet excited state  $|S_1; \nu_v = \mathbf{0}, \nu_p = \mathbf{0}\rangle$  due to fast vibrational relaxation. This is known as *Kasha's rule* [53]. The most prominent of such transitions occurs between  $|S_1; \nu_v = \mathbf{0}, \nu_p = \mathbf{0}\rangle$  and the ground state  $|S_0; \nu_v = \mathbf{0}, \nu_p = \mathbf{0}\rangle$  as a result of large wavefunction overlap, i.e., small Huang-Rhys factors of vibron and phonon states. This transition is re-

ferred to as the 00-zero-phonon line, abbreviated as ZPL in the following discussion. Due to coupling with the vibrational degrees of freedom, the ZPL transition strength is reduced compared to that of a perfect two-level system by a factor related to the Franck-Condon factors of each intramolecular and intermolecular vibrational modes in the host-guest system. The latter is called the *Debye-Waller factor* and is temperature-dependent due to low-frequency phonons involved [46]. For a number of PAH molecules [see Fig. 2(b)], the ZPL transition lies in the visible to near-infrared frequency range, making them favorable for quantum optics experiments. At liquid helium temperatures and with appropriately chosen host matrices, the ZPL transition can narrow to near its lifetime limit. This benefits from the non-polar nature of the electronic wavefunction. It is worth noting that the insertion into a host matrix can slightly break the centrosymmetry, thereby inducing a net electric dipole [43] and altering the vibrational mode structure [21]. Above liquid helium temperatures, the electron-phonon coupling leads to a reduction in the ZPL strength in addition to a decrease in the Debye-Waller factor as a result of elastic electron-phonon scatterings, known as *pure dephasing* [54].

In summary, a single molecule embedded in a solid-state host exhibits a rich energy structure supporting a multitude of well-defined transitions ranging from radio to optical frequencies. Next, we delve into the details of these molecular degrees of freedom and discuss their quantum mechanical character.

## B. Vibrational States

The optomechanical character of molecules was first discovered by Raman [55], as the optical excitation of molecules yields light scattering to new frequencies determined by the intramolecular vibrational energies. In the context of molecular quantum optics, this optomechanical character has traditionally been regarded as a source of decoherence due to fast vibrational relaxation processes. Yet, if vibrational states can be engineered to have long lifetimes, they could be exploited as a resource in quantum technologies.

### 1. Intermolecular Vibrational States

The typical vibrational landscape of a molecular host-guest system is shown with an example of a perylene-doped naphthalene and anthracene crystal in Fig. 3(a), where the phonon density of states in naphthalene crystal (red lines), anthracene crystal (black lines) and intramolecular vibrations of a perylene molecule (green lines) are plotted up to 12 THz. Among many mechanical degrees of freedom, phonons corresponding to the center-of-mass translational motion of host molecules are the lowest in energy scale. These modes approximately span

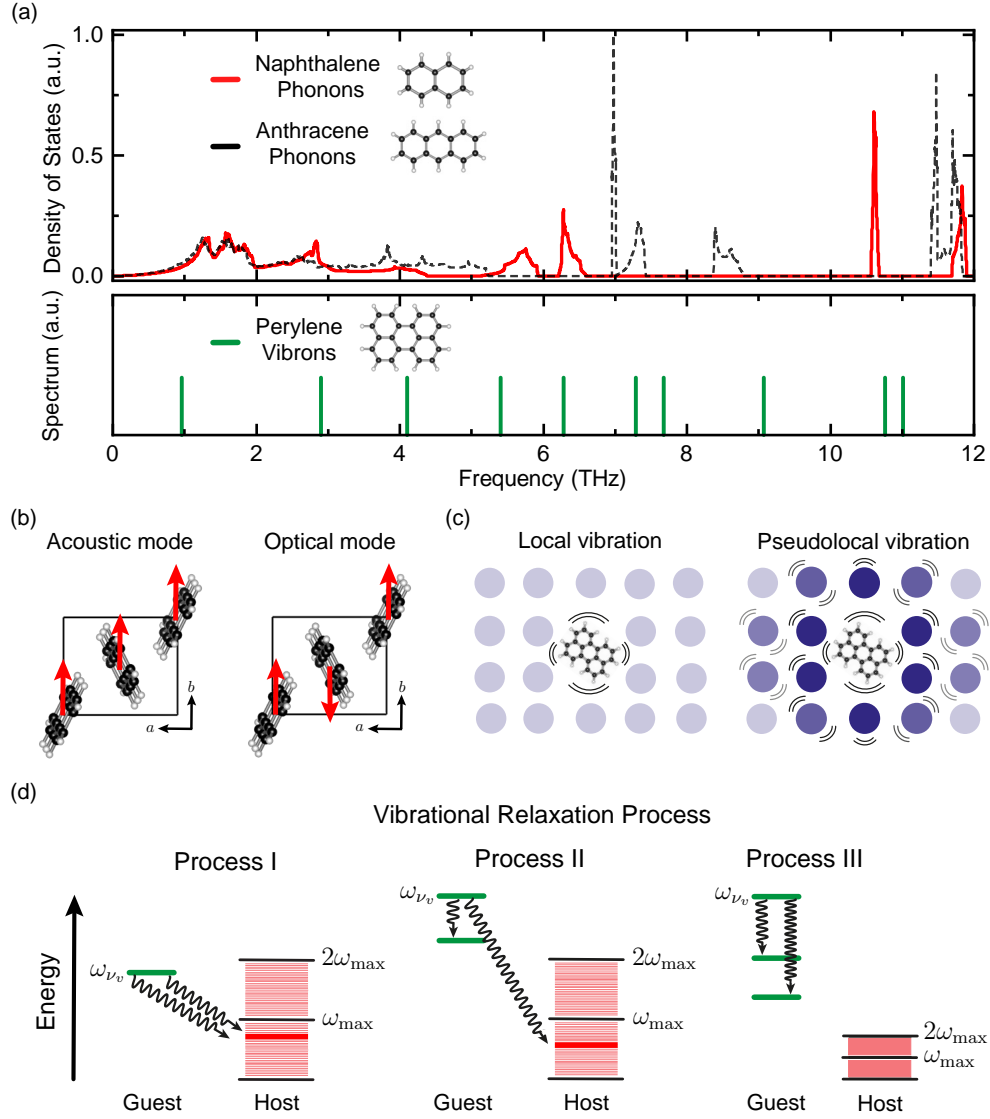


FIG. 3. (a) Phonon density of states (DOS) of naphthalene, and anthracene crystal (top) and intramolecular vibrations of a perylene molecule (bottom), shown by red, black and green lines, respectively. The *ab initio* calculations are done using Vienna Ab initio Simulation Package [56–59] with Perdew-Burke-Ernzerhof functional [60] and Tkatchenko-Scheffler dispersion correction [61]. We used phonopy to calculate the phonon DOS for a  $2 \times 4 \times 2$  supercell [62] (b, c) Schematics for the acoustic and optical phonon of an anthracene crystal and pseudolocal mode of the host-guest system. The crystal axes are denoted by  $a$  and  $b$ , respectively. (d) Vibrational relaxation mechanisms for an intramolecular vibration of a guest molecule in a host environment.  $\omega_{\nu_v}$  and  $\omega_{\max}$  denote the intramolecular vibrational frequency of the state  $|S_0; [0, \dots, 0, 1, 0, \dots, 0], \nu_p = \mathbf{0}\rangle$  and maximal phonon frequency in the host matrix, respectively.

the frequency range 0 – 4.5 THz with a cut-off frequency determined by the unit-cell size of the host molecular crystal, i.e., around 1 nm for PAH molecular crystals. Assuming molecules as rigid bodies, there are  $3N - 6$  lattice modes for  $N$  number of molecules in the crystal, which practically renders the spectrum of such modes as a continuum. These modes can be classified as acoustic and optical phonons based on their properties at the zero-phonon wavevector. Acoustic phonons result from in-phase motion of molecules as rigid bodies and their frequencies range in between 0 – 1.5 THz for PAH molecular

crystals [see Fig. 3(b)]. These modes possess linear dispersion for low frequencies, i.e., up to  $\sim 100 - 200$  GHz, which results in a small density of states. The lifetime of these modes is determined by absorption and boundary scattering effects and can reach up to millisecond timescales for modes up to megahertz frequencies [52]. However, the electron-phonon couplings to these modes are small due to large phonon mode volumes in the molecular crystal [38]. Hence, optically accessing these modes is difficult.

Besides, high-frequency acoustic phonons and optical

phonons have nonlinear dispersion relations with low group velocities, and correspond to out-of-phase motion of molecules in the unit-cell [see Fig. 3(b)]. These modes typically have lifetimes in the order of picoseconds due to the decay into acoustic modes at lower frequencies [63]. They have considerable electron-phonon coupling strengths and hence constitute approximately 10% of the overall light scattering for typical host-guest systems at liquid helium temperatures [46]. The transitions to these states are visible in the phonon-wing spectra whose probability peaks at around 1.5 – 2 THz and gradually decays towards the maximal phonon frequencies. Such a low optical excitation probability at high frequencies stems from low phonon DOS and the size of the guest molecule, i.e., its electron density in  $k$ -space [64]. Due to their high densities and fast vibrational relaxations, these states are typically considered as a bath in molecular quantum optics [38].

The phonon density of states possesses several other band structures at higher frequencies compared to  $\omega_{\max}$ , i.e.,  $> 4.5$  THz, which corresponds to the librational and rotational motions of individual lattice molecules [65]. For anthracene and larger PAH molecular crystals, low-frequency phonons of such character are amalgamated into the continuum of phonons, and extend their cut-off frequency [66], as shown in Fig. 3(a). As argued above, the electron-phonon couplings to such modes are less probable due to the cut-off frequency induced by the electron density in  $k$ -space and hence play a minor role in molecular host-guest systems.

## 2. Intramolecular Vibrational States

The molecular host-guest system additionally possesses intramolecular vibrations of the guest molecule [see Fig. 3(a)]. There are  $3n - 6$  vibrations corresponding to  $n$  number of atoms in the molecule, and they correspond to librational and bond vibrations of the guest molecule, reaching up to 93 THz for the C-H stretching motion. Frequencies of librational modes are determined by the size of the molecule. The lowest libration frequency for perylene molecule in vacuum is 0.9 THz. In the range of 0 – 5 THz, librational modes of the guest molecule hybridize with the translational lattice modes. This results in slightly delocalized vibrational states over the host molecules, so-called *pseudolocal phonon modes* [67] [see Fig. 3(c)]. Depending on the insertion of the guest molecule, some of these modes are Raman (Franck-Condon) active, and due to the semi-localized nature of their vibration over the guest molecule, they can have large electron-vibron coupling strengths compared to phonon modes of the host matrix. This is evident in the single molecule emission spectra, where the phonon-wing spectrum shows pronounced Lorentzian peaks below 5 THz with lifetimes in the order of picoseconds [68]. In addition, these modes are shown to be responsible for temperature-dependent line broad-

ening of the ZPL transition [54].

The rest of the intramolecular vibrations are localized on the guest molecule as the host vibrational density of states is sparse [see Figs. 3(a, c)]. Hence, these modes have very large electron-vibron coupling strengths in the order of their frequencies [42, 46, 69]. Such ultra-strong couplings can be witnessed from the emission/absorption spectrum of the host-guest system.

## 3. Vibrational Relaxation

Despite long radiative lifetimes of molecular vibrations in the gas phase that range up to seconds [70, 71], the nonradiative vibrational relaxation in a solid typically yields lifetimes in the order of picosecond irrespective of the frequency and temperature range [69]. This process stems from the anharmonicity of the potential energy surface along host and guest vibrational coordinates, and results in short vibrational lifetimes even though certain vibrations of the guest molecule are in principle mechanically shielded due to gaps in the host vibrational band [see Fig. 3(a)]. Based on the perturbative treatment of this problem, the vibrational relaxation process due to cubic anharmonic interactions between vibrational modes can be divided into three categories depending on the frequency of the guest vibrational mode ( $\omega_{\nu_v}$ ) [72], as shown in Fig. 3(d). In the first process, the guest molecule's vibrational frequency is smaller than two times the phonon cut-off frequency ( $\omega_{\max}$ ), i.e., cut-off frequency of the two-phonon density of states, such that the vibration of the guest molecule relaxes via two lattice phonons based on energy and momentum conservation as a result of the three-body interaction between the normal-mode displacements. The second process happens when the guest molecule's vibrational frequency lies above the cut-off frequency of the two-phonon density of states, where an intramolecular vibration of the guest molecule could assist the non-radiative relaxation. If the guest molecule's vibrational frequency is too large compared to the phonon cut-off frequency, the vibrational relaxation occurs via intramolecular relaxation in the guest molecule as the third process. Besides, as this picture is perturbative, the higher-order anharmonicities between vibrational modes also play a role once the energy conservation cannot be satisfied via relaxation to two vibrations. As a result, despite the weak-couplings between the intramolecular guest vibrations and phonon modes, the immense number of decay paths provided by the continuum of phonon modes yield picosecond-scale vibrational lifetimes. Despite such a short lifetimes, these vibrations are mostly in their quantum ground state even at room temperature, an interesting property that could be exploited to push quantum technologies to room temperature [34, 73].



### C. Spin states

The spin states of electrons and nuclei in the molecular host-guest system offer additional parameter spaces that hold potential for quantum applications. We start by introducing the properties of the lowest triplet state  $|T_1; \nu_v = \mathbf{0}, \nu_p = \mathbf{0}\rangle$  and its role in the photophysics of the molecule.

In the  $|T_1; \nu_v = \mathbf{0}, \nu_p = \mathbf{0}\rangle$  state, the two unpaired electrons interact through the magnetic dipole-dipole interaction, which can be described by the phenomenological model Hamiltonian  $\mathbf{H}_{\text{ZFS}} = \mathbf{S} \cdot \mathbf{D} \cdot \mathbf{S}$ , with  $\mathbf{S}$  the total spin operator and  $\mathbf{D}$  the fine-structure tensor [74]. For PAH molecules with  $D_{2h}$  symmetry, such as pentacene and perylene,  $\mathbf{D}$  can be diagonalized in the coordinate system defined by the geometrical symmetry axes  $\alpha = x, y, z$  of the molecule, as illustrated with a perylene molecule in Fig. 4(a). The three eigenstates associated with the three principal vectors, known as the *zero-field eigenstates*, can be labeled  $|T_1^\alpha\rangle$ . In  $|T_1^\alpha\rangle$ , the magnetic moment of the electron spin is oriented in the plane perpendicular to the axis  $\alpha$ . As shown in Fig. 4(b), the ZFS is characterized by two parameters  $D$  and  $E$ , which correlate with the delocalization of the spin density in the  $\pi$  orbital and the axial symmetry of the molecule, respectively. Transitions between any pair of the zero-field states are allowed by magnetic-dipole interactions and can be driven by microwave fields [74].

In the triplet manifolds, the electron spin couples to nuclear spin wavefunction  $\phi_{\text{nuc}}(\mathbf{I})$  through the hyperfine interaction. This interaction is described by the Hamiltonian  $\mathbf{H}_{\text{HFI}} = \sum_i \mathbf{S} \cdot \mathbf{A}^{(i)} \cdot \mathbf{I}_i$ , where  $\mathbf{I}_i$  is the nuclear magnetic moment of the  $i^{\text{th}}$  nucleus, and  $\mathbf{A}^{(i)}$  is its hyperfine interaction tensor with the electron spin. In hydrocarbon molecular crystals, nuclear spins mainly originate from protons and  $^{13}\text{C}$  isotopes in the guest molecule and the host matrix. Notably, protons can be replaced by deuterons via isotope exchange reactions, through which the number of spin-1/2 nuclei in the guest molecule and the matrix can be significantly reduced. Using deuterated matrices makes it possible to resolve the hyperfine splitting due to individual nuclear spins in the molecule [75, 76]. The right panel of Fig. 4(b) illustrates the hyperfine splitting with a magnetic field applied along the  $z$  axis and considering only a single spin-1/2 nucleus in a perylene molecule. Similar to the demonstration with nitrogen-vacancy centers in diamond [77], hyperfine splitting offers the opportunity to selectively access individual nuclear spin states using narrow-band microwave pulses, and facilitate the realization of controlled-rotation gates between electron and nuclear spins [77].

The triplet state can be populated through optical pumping on the ZPL transition. From the  $|S_1; \nu_v = \mathbf{0}, \nu_p = \mathbf{0}\rangle$  state, the molecule can occasionally cross over to a vibrationally excited level in the triplet manifold  $|T_j; \nu_v \neq \mathbf{0}, \nu_p \neq \mathbf{0}\rangle$ . This process, known as *intersystem crossing* (ISC), is weakly allowed due to spin-orbital coupling, and typically assisted by intermolecular

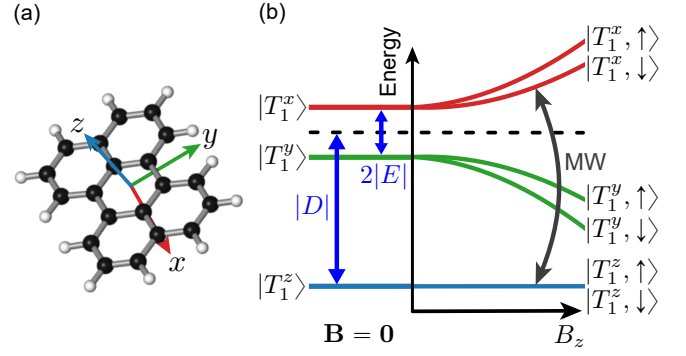


FIG. 4. (a) Structure of a perylene molecule and its three symmetry axes. (b) Left: Zero-field splitting of the three triplet sublevels  $|T_1^\alpha\rangle$  in the absence of an external magnetic field ( $\mathbf{B} = 0$ ), characterized by parameters  $D$  and  $E$ . Right: Zeemann shift and hyperfine splitting due to a spin-1/2 nuclear spin, when an external magnetic field  $B_z$  is applied along the  $z$  axis. In the regime of a weak magnetic field, the zero-field bases  $|T_1^\alpha\rangle$  are still approximated eigenstates of the electron spin and  $|\uparrow\rangle, |\downarrow\rangle$  denote the two states of the nuclear spin. Microwave (MW) driving of the electron spin enables controlled-rotation gates, conditioned on the state of the nuclear spin.

and intramolecular vibrations [78]. Following ISC, the molecule undergoes nonradiative relaxation and reaches the lowest triplet state  $|T_1; \nu_v = \mathbf{0}, \nu_p = \mathbf{0}\rangle$ . The rate of ISC also depends on the final spin sublevel  $|T_1^\alpha\rangle$  of the triplet manifold [44]. From the state  $|T_1; \nu_v = \mathbf{0}, \nu_p = \mathbf{0}\rangle$ , the molecule can decay to the ground state manifold either via phosphorescence, or through ISC to a  $|S_0; \nu_v \neq \mathbf{0}, \nu_p \neq \mathbf{0}\rangle$  level followed by vibrational relaxation. These two processes compete with each other. The rate of ISC has been shown to follow the energy-gap law [79], while its underlying microscopic mechanisms are generally complex [80]. Since both processes are spin-forbidden, the lifetime of the  $|T_1; \nu_v = \mathbf{0}, \nu_p = \mathbf{0}\rangle$  state is long, reaching up to seconds [81].

In the triplet state, the molecule does not fluoresce, so a decrease in fluorescence intensity can serve as an indicator of triplet-state occupation. By using a resonant microwave drive to shuffle the population between two of the three sub-levels, the mean residence time in the triplet state can be altered, resulting in changes to the steady-state fluorescence intensity. This technique was applied to pentacene molecules in *para*-terphenyl crystal in the 1990s, which led to the first detections of electron spin transitions in a single molecule [82, 83]. These efforts were later extended to deuterated pentacene molecules and enabled the spectroscopic detection of the hyperfine splittings due to individual  $^{13}\text{C}$  and proton spins [75, 76]. Very recently, the detection and coherent control of triplet electron spins have been demonstrated on an ensemble of pentacene molecules at room temperature [39], potentially setting the ground for ambient quantum sensing using molecular host-guest mate-

rials.

### III. PERSPECTIVES IN QUANTUM TECHNOLOGY

So far, single organic molecules have found applications as single photon sources [6, 7], quantum optical nonlinear elements [8–10], and nanoscale sensors for probing local field properties in materials [15, 31]. They have also been integrated into nanophotonic and hybrid nanostructures, such as nanoantennas, waveguides and optical resonators, laying out promising future paths in photonic quantum technologies [3]. The vibrational and spin states of molecular host-guest systems, as discussed in the previous section, hold significant potential for expanding the application of these systems. Furthermore, the chemical diversity of molecules could enhance this potential by providing molecular candidates with tailored quantum properties. In the following, we outline possible strategies to harness the vibrational and spin states for applications that have not been realized on these systems before and discuss the opportunities presented by the vast chemical space.

#### A. Vibrational quantum memory

A quantum memory enables the storage of quantum information and plays a pivotal role in quantum computing and communication [84]. Among the multitude of energy levels in a single molecule, the vibrational degrees of freedom can potentially be harnessed for quantum memories.

The schematic of a vibrational quantum memory in a single molecule is shown in Fig. 5, where the molecular electronic transition provides the interface to flying qubits and quantum memory is realized in the ground state vibrational manifold. The flying qubits encoded in photon-number [85] or time-bin degrees of freedom [86] can be stored and retrieved with well-established techniques such as stimulated Raman scattering [38, 87] as shown in Fig. 5 or stimulated Raman adiabatic passage [88] or heralded Stokes Raman scattering [85]. Despite the sizable couplings between the electronic and vibrational levels, the picosecond-timescale vibrational lifetimes in these systems limit such applications. Although the vibrational relaxation mechanism is challenging to control in the solid state, it has recently been proposed that low-frequency acoustic phonon modes in the host crystal can be harnessed as quantum memory elements once the molecular environment is engineered [38]. These so-called continuum modes can be made spectrally resolved by employing nanometer-sized host crystals, compatible with state-of-the-art fabrication techniques [89, 90]. In addition, the lifetimes of these phonon modes can be made long-lived up to milliseconds via phononic crystal engineering techniques. Although such a quantum memory operates at millikelvin

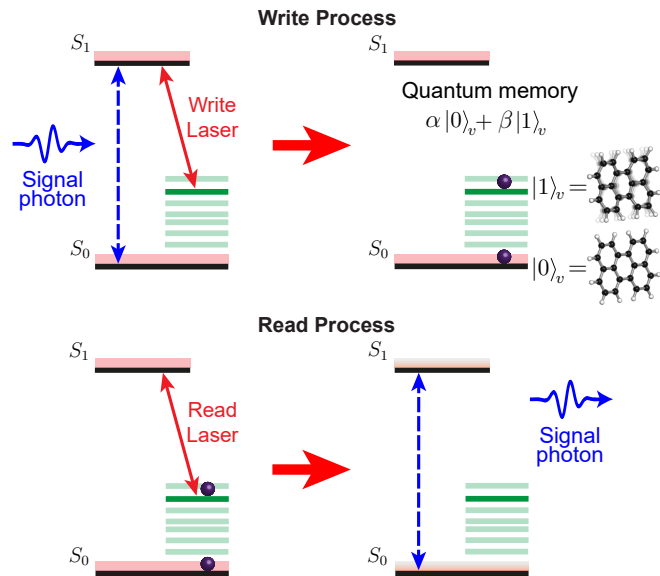


FIG. 5. Schematics showing photonic quantum memory operation via stimulated Raman scattering process. Flying qubits are interfaced to the ZPL transition ( $|S_0; \nu_v = 0, \nu_p = 0\rangle - |S_1; \nu_v = 0, \nu_p = 0\rangle$ ) shown with the dashed blue arrows and mapped into (from) the vibrational state with write (read) laser show with the red arrows. The vibrational states of a single molecule in the ground state manifold  $|0\rangle_v$  and  $|1\rangle_v$  act as a quantum memory. Here,  $|0\rangle_v$  and  $|1\rangle_v$  are short hand notations for  $|S_0; \nu_v, \nu_p = 0\rangle$  and  $|S_0; [0, \dots, 0, 1, 0, \dots, 0], \nu_p = 0\rangle$ , respectively. The schema is also valid for phonon states [38].

temperatures due to the low phonon frequencies involved, the higher frequency vibrations such as optical phonons in the host matrix and intramolecular vibrations of the guest molecule could be utilized to realize quantum memory elements operating at high temperatures once their decay paths are controlled. The latter could be achieved by choosing host materials with a sparse vibrational density of states such as benzene or by placing small molecules on a surface vibrationally decoupled from the substrate beneath [91].

#### B. Molecular optomechanics

The optical and mechanical degrees of freedom are weakly interacting beyond systems at the atomic scale due to the large mechanical mass and small momentum of optical beams. In the last decade, highly cooperative interactions between those have been made possible by utilizing engineered optomechanical cavities with low optical and mechanical losses [92]. These efficient interactions enabled precise control and manipulation of mechanical motion with light, and hold promises for quantum sensing, signal transduction, and so on [93].

Analogous to the conventional optomechanical setups, a single-molecule host-guest system offers optomechan-



ical interactions thanks to the inherent couplings between their optically accessible electronic and vibrational transitions. The molecular system provides such couplings across a very wide frequency range spanning kHz to THz. Importantly, the electron-vibration coupling strengths can reach values larger than the mechanical oscillation frequencies, putting the molecular system into the ultra-strong optomechanical coupling regime at the single-photon level [46]. This nonlinear quantum optomechanical regime has not been reached in solid-state cavity optomechanical setups so far [92]. In addition, due to the extremely large quality factors of the electronic transitions in the order of  $10^7$ , these molecular systems could also ensure a path to access large quantum optomechanical cooperativities, i.e.  $C_{\text{opt}} = 4g^2/\bar{n}\kappa_v\gamma_0$  [94], where  $\bar{n}$  denotes the thermal population of the vibrational mode,  $\kappa_v$  and  $\gamma_0$  denotes the vibrational and electronic excited state decay rates, respectively. Reaching such a high cooperativity regime in cavity optomechanical systems is challenging due to parasitic optical absorption [94], which is negligible in molecular systems. Hence, single molecules can facilitate quantum optomechanical applications such as coherent frequency conversion between photons [95] which is essential for quantum information processing [96].

In typical single-molecule host-guest systems, the efficient optomechanical interactions suffer from the fast vibrational relaxations as the quantum character of these levels is lost in the timescale of electron-vibration couplings. Therefore, it is important to control vibrational relaxation rates. Such a control can be done for acoustic phonons as in traditional cavity optomechanical setups, where techniques like impedance mismatch or phononic bandgap structuring can be used to decouple certain acoustic modes from their environment. For anthracene crystal doped with dibenzoterrylene, it has been proposed that efficient optomechanical interactions are at reach by using appropriately designed phononic structures [38]. On the other hand, it is a great challenge to extend such a control to optical phonons and guest molecular vibrations as discussed in Section II B. Considering their significant electron-vibration coupling strengths and non-negligible thermal populations even at room temperature, engineering such long-lived states could lead to efficient optomechanical applications at elevated temperatures. This approach also offers the potential to explore previously inaccessible regimes in optomechanical and nonequilibrium condensed-matter systems.

### C. Spin-photon interface

The spin states are long-lived and well-isolated from their environment, making them attractive candidates as quantum memory units. Additionally, the excellent properties of molecular ZPL emission offers the possibility to coherently interface spins with propagating photons. These two features combined make it possible to

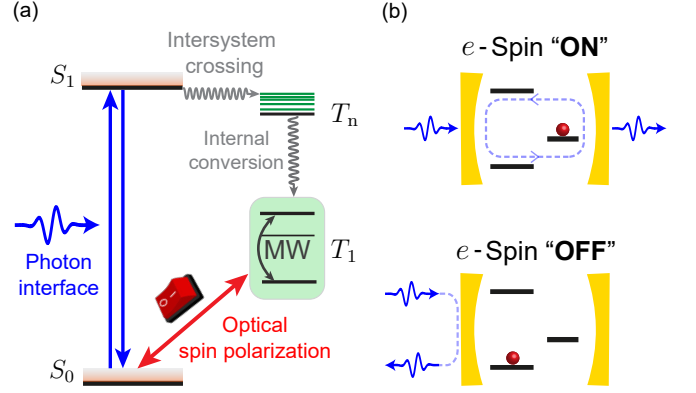


FIG. 6. (a) Achieving optical manipulation of the singlet-triplet transition will provide a “switch” to control the electron spin, allowing it to be turned “on” and “off” on demand. (b) This capability combined with coherent photon scattering via the  $|S_0; \nu_v = 0, \nu_p = 0\rangle$  to  $|S_1; \nu_v = 0, \nu_p = 0\rangle$  ZPL transition facilitates optical interfacing of the electron spin. Illustrated is a spin-controlled photon transmission through a cavity, whose frequency is set resonant to the ZPL transition.

realize a molecular spin-photon interface, which can serve as a key component for quantum networks [97].

To realize a coherent spin-photon interface, it is necessary not only to have optically addressable spin states but also to achieve an efficient collection of lifetime-limited photons into a single optical mode. For solid-state emitters, the efficiency of detecting such lifetime-limited photons is constrained by the emitter’s internal quantum efficiency, the branching ratio of ZPL emission, and the optical dephasing rate. An established approach to mitigate these limitations is through resonant coupling with an optical cavity [98]. PAH molecules are particularly promising in this regard due to their high quantum efficiency, close to lifetime-limited ZPL emission, and relatively high branching ratio. Recent advances in cavity-based interfaces have achieved strong coupling between the ZPL transition of a single molecule and a tunable Fabry-Perot microcavity [10, 99], laying the groundwork for the realization of a molecular spin-photon interface.

Figure 6(a) illustrates a possible scheme of a molecular spin-photon interface. To entangle the electron spin with photons, one would need to prepare the molecule in a superposition of  $|S_0; \nu_v = 0, \nu_p = 0\rangle$  and a sublevel of  $|T_1; \nu_v = 0, \nu_p = 0\rangle$ . This can in principle be achieved using a narrow linewidth laser to coherently drive the transition between these two states. The  $|S_0; \nu_v = 0, \nu_p = 0\rangle$  to  $|S_1; \nu_v = 0, \nu_p = 0\rangle$  transition is strongly coupled to an optical microcavity and serves as an optical interface. Depending on the state of the molecule, a photon with its frequency matching the undressed cavity frequency will either reflects off from the cavity, due to the vacuum Rabi splitting [10] when the molecule is in  $|S_0; \nu_v = 0, \nu_p = 0\rangle$ , or transmits through the cavity when the molecule is in  $|T_1; \nu_v = 0, \nu_p = 0\rangle$  (considering a symmetric mirror

configuration). Thus the internal state of the molecule becomes entangled with the spatial mode of the photon.

A critical step in this scheme is the optical addressing of singlet-triplet transition in a single molecule. Such transitions have been studied in experiments with cold alkaline earth atoms, e.g., strontium, and utilized for optical clocks transitions [100]. In recent years, singlet-triplet transitions have been measured on diatomic molecules in the gas phase [101, 102]. Optical excitation of singlet-triplet transitions in a single solid-state emitter has not been demonstrated. The challenges are mainly technical. First, in planar molecules without heavy metal atoms, the spin-orbit coupling is rather weak, leading to long lifetimes and thus narrow transition linewidths. Second, the exact frequencies of these transitions are difficult to predict, and the matrix introduces shifts to the transition frequency compared to that of a molecule in vacuum. In addition, considerations need to be taken in identifying molecular candidates for such an investigation. We will discuss possible molecular candidates in Section III E.

#### D. Molecular spin register

A quantum register represents a collection of individual qubits, grouped to serve as a basic component for information processing. The molecular framework offers an attractive route for constructing chemically configurable registers of nuclear spins. Depending on the number of active nuclear spins, two operation regimes can be interesting. First, a small ensemble of 10 – 20 protons coupled to a single electron spin, which is naturally provided by a PAH molecule, constitutes a well-defined *central-spin system*. Such a system offers extensive possibilities to harness the collective spin states for quantum memory [103, 104] and decoherence protection [105]. Along this route, highly efficient dynamic polarization of nuclear spins has been achieved on pentacene molecules doped in naphthalene hosts, showing remarkably long relaxation times of over 900 hours [106, 107]. The know-how in these experiments can be transferred to realize quantum control of collective spin states at the single molecular level. In the second regime, a register of a few addressable spin-1/2 nuclei, realized through e.g., partial deuteration of the molecule, could provide a platform where the state of individual nuclei spins can be detected and manipulated independently. This can be made possible using microwave pulses to perform conditional gates between the electron and nuclear spin, similar to the experiments performed on color centers in diamond [77]. It is worth noting that pairs of chemically identical  $^{13}\text{C}$  spins in a deuterated pentacene molecule have been spectrally resolved in optically detected magnetic resonance measurements [108]. Their significantly narrowed transition linewidth indicates an efficient decoupling from the environment. Such a “dark” state of a pair of chemically identical nuclei is highly promising for decoherence-protected encoding schemes [109].

Apart from nuclear spin qubits, using nuclei with larger spin quantum numbers can extend the system to a qudit (a system with a  $d$  number of levels) register. Nuclear spins with higher multiplicity offer an interesting route for quantum information processing beyond qubit-based approaches [110]. They are predicted to bring along reduced numbers of physical quantum units and gate operations for accomplishing a certain computing task. A parallel line of research on molecular qudits is being pursued in the context of molecular nanomagnets [110]. On the PAH platform, it is readily feasible to incorporate a defined number of spin-1 nuclei, e.g.,  $^{15}\text{N}$ , through bay functionalization with imide groups [111]. Along this line, perylenediimide and terrylenediimide derivatives have already been studied in single-molecule optical spectroscopy [112, 113].

Overall, the molecular framework provides the capability to integrate electron spin, nuclear spins, and optical interfaces within a single platform. In addition to the tailorability by chemical modification, a particularly appealing aspect of this system is the metastable triplet state. Once optical driving of such a transition is realized, it enables a deterministic control to switch “on” and “off” the electron spin [see red arrow in Fig. 6(a)]. This feature is particularly compelling, given that the electron spin acts as a significant source of decoherence for the nuclear spins [114]. By enabling a deterministic on-off switch of the hyperfine interaction, this system can address the trade-off between gate time and susceptibility to decoherence, further enhancing the utility of the molecular platform.

#### E. Exploiting the Chemical Space

Having introduced the potential of vibrational and spin states within the molecular host-guest system, we now extend the discussion to another research line that remains largely unexplored, namely the molecular candidates within the broader chemical space. Previous achievements in molecular quantum optics have relied on a handful of molecule-host combinations that are identified based on intuition and processes of trial and error. The chemical space of molecules involves more than a billion species [126], offering enormous potential to provide molecules with a wide range of desirable properties.

We provide a glimpse into the chemical space of molecules in Fig. 7, where 26 centrosymmetric PAH molecules containing up to 26 carbon atoms are identified from the NIST database [115]. Their singlet-singlet ( $|S_0; \nu_v = 0, \nu_p = 0\rangle - |S_1; \nu_v = 0, \nu_p = 0\rangle$ ) and singlet-triplet ( $|S_0; \nu_v = 0, \nu_p = 0\rangle - |T_1; \nu_v = 0, \nu_p = 0\rangle$ ) vertical transition energies are calculated using *ab initio* methods at the level of coupled-cluster theory with single and double excitations (CCSD) [123] and plotted versus each other. Note that these energies do not include salvation effects or zero-point energy correction stemming from the vibrational degrees of freedom. The results show

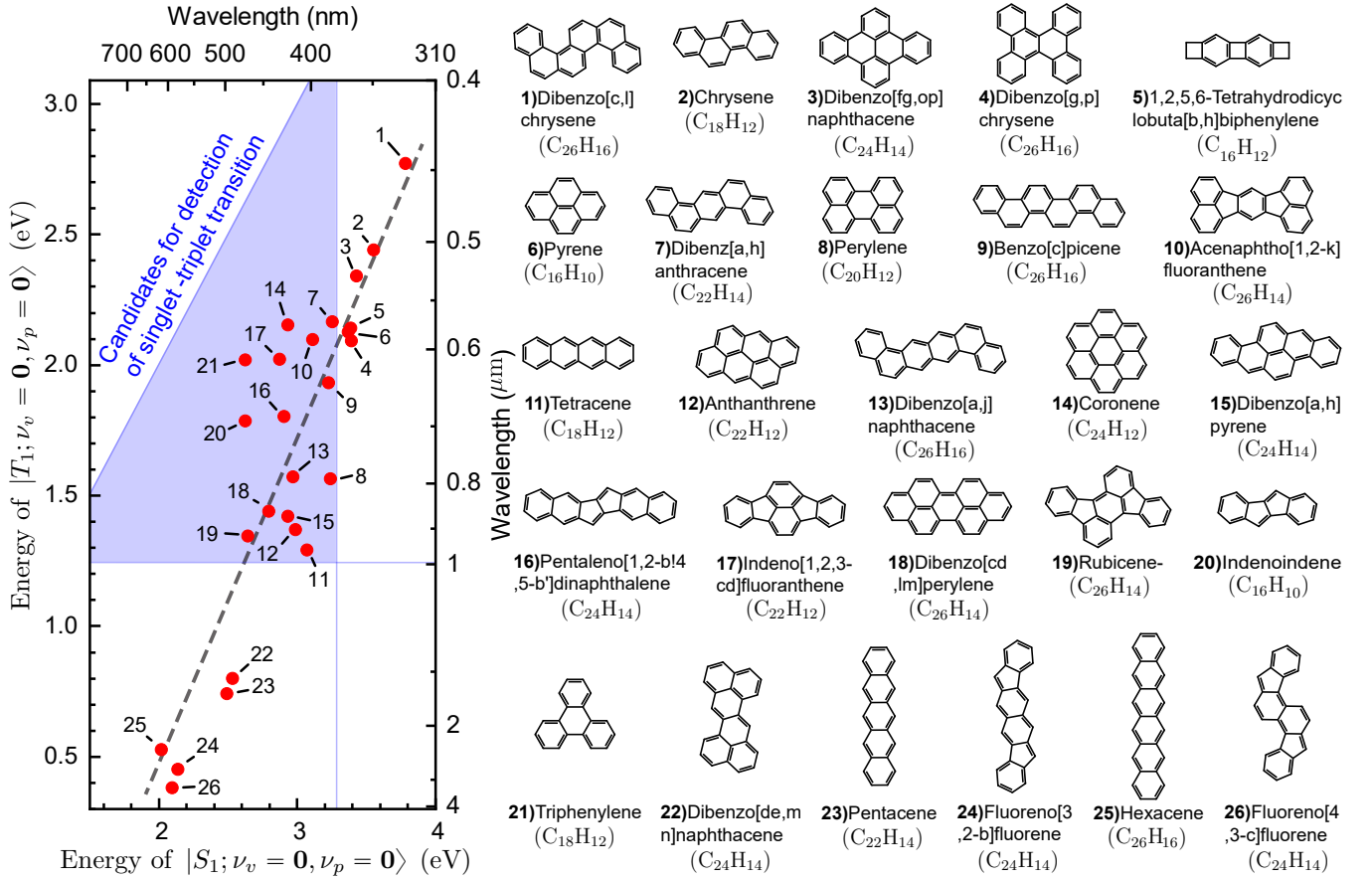


FIG. 7. The computed vertical excitation energies of  $|S_1; \nu_v = 0, \nu_p = 0\rangle$  and  $|T_1; \nu_v = 0, \nu_p = 0\rangle$  of all centrosymmetric PAHs containing up to 26 carbon atoms found in the NIST Chemistry WebBook [115]. The ground state geometry optimizations are performed at the DFT level with B3LYP functional [116–118], def2-TZVP basis set [119] with its auxiliary basis set [120] and the D3 dispersion correction [121, 122]. The vertical excitation energies are calculated using DLPNO-STEOM-CCSD method with def2-TZVP basis set [123, 124]. The molecular candidates suitable for the optical detection of  $|S_0; \nu_v = 0, \nu_p = 0\rangle - |T_1; \nu_v = 0, \nu_p = 0\rangle$  transition are highlighted by the blue-shaded area. The grey dashed line is a guide to an eye for the linear scaling between vertical excitation energies. The simulations are carried out via ORCA program, v.5.0. [125].

an approximately linear scaling behavior between the singlet-singlet and singlet-triplet transition energies (see dashed black line in Fig. 7), spanning a large range in the visible and near-infrared spectrum. This molecular space has not been studied at the single-molecule level except for perylene and pentacene. We discuss the potential of such a diverse chemical space with two possible applications.

(i) The large variety of  $|S_0; \nu_v = 0, \nu_p = 0\rangle - |S_1; \nu_v = 0, \nu_p = 0\rangle$  transition energies of these molecules offers possibilities to engineer single photon sources with on-demand emission frequencies across the visible spectrum. Although the identified molecules do not cover the entire range, the wavelength gaps between them could be bridged using several strategies. First, chemical modifications, such as deuterium and fluorine substitution of protons, or the adaption of imide or anhydride groups, can shift the center emission wavelength by up to  $\sim 50$  nm [112, 113, 127]. Second, selecting different host matrices or different insertion sites in a host can affect

the emission wavelength by up to 20 nm [128]. Third, within a given host matrix, the center of inhomogeneous broadening can be tuned with the thickness of the host crystal, providing an accessible frequency range of several nanometers [129]. Fourth, the inhomogeneous broadening of ZPL frequencies can span over  $\sim 1$  nm, allowing spectral selection of molecules within this frequency range. Finally, fine adjusting of the ZPL emission frequency can be achieved through the Stark effect, with a tuning range of  $\sim 500$  GHz [12].

(ii) The molecules in Fig. 7 also offers a valuable chemical space for identifying molecular candidates suitable for realizing spin-photon interfaces, where the optical addressing of the singlet-triplet transition is essential but remains an ongoing challenge [128]. Molecules suitable for addressing singlet-triplet transitions should meet two conditions regarding their transition energy: First, the energy-gap law predicts that a lower energy of  $|T_1; \nu_v = 0, \nu_p = 0\rangle$  is associated with a larger non-radiative ISC rate [79]. Therefore, molecules with

a higher  $|T_1; \nu_v = \mathbf{0}, \nu_p = \mathbf{0}\rangle$  energy are more favorable. Second, since the energy of  $|T_1; \nu_v = \mathbf{0}, \nu_p = \mathbf{0}\rangle$  is lower than that of  $|S_1; \nu_v = \mathbf{0}, \nu_p = \mathbf{0}\rangle$ , a high energy of  $|S_1; \nu_v = \mathbf{0}, \nu_p = \mathbf{0}\rangle$  poses challenges. This makes it difficult to find suitable host materials and necessitates widely tunable laser sources in the ultraviolet, which is technically demanding. Therefore, one would aim for molecules with a high  $|T_1; \nu_v = \mathbf{0}, \nu_p = \mathbf{0}\rangle$  energy but with a relatively small energy gap to the  $|S_1; \nu_v = \mathbf{0}, \nu_p = \mathbf{0}\rangle$  state. These two criteria let us constraint the selection of guest molecules into the subspace illustrated by the blue-shaded area in Fig. 7.

These two examples are just a glimpse of the immense possibilities provided by the chemical space. A larger chemical space can be screened in the future using machine learning strategies in theoretical [130] or experimental settings [131] to identify new host and guest combinations with specific properties such as ZPL frequency at telecom wavelengths, long vibrational lifetimes, large electron-vibration coupling strengths or spin coherence times. Eventually, inverse molecular design techniques [126] can be employed to create new molecules with tailored photonic, vibronic, and spin properties, unleashing the full power of chemical synthesis. These approaches could drive advances beyond traditional intuitive chemical design principles and accelerate the development of molecules for quantum technologies.

#### IV. OPEN CHALLENGES

Several challenges need to be addressed both in theory and in experiment to unlock the potential of molecular host-guest systems discussed above. Here, we iterate on three major challenges that we identify from state-of-the-art understandings.

First, advancing solid-state molecular quantum technology requires a deeper understanding of molecule–host interactions from first principles. Static interactions, such as the insertion of a single molecule into the host matrix, which influence ZPL frequencies and vibrational properties, can often be addressed through full or semi-classical simulations [132–135]. However, current studies remain far from being quantitative due to the inherent inhomogeneity of local molecular environments [69]. Meanwhile, dynamical interactions including spectral diffusion, pure dephasing, non-radiative relaxations, and fluorescence blinking pose additional challenges, as they critically affect the optical properties of single molecules in the solid state by introducing decoherence [136]. These interactions not only hinder the exploitation of all molecular degrees of freedom but also constrain the choice of suitable host materials. A comprehensive understanding and characterization of such interactions are therefore key to the development of controllable and scalable molecular quantum technologies. However, modeling these interactions is particularly challenging due to the involvement of multiple degrees of freedom and

their wide energy scales. Addressing this multi-scale problem requires a multidisciplinary approach that integrates tools from condensed matter theory and physical chemistry, including first-principles calculations and model systems. These theoretical efforts must also be supported by dedicated experiments to reveal the microscopic dynamics governing these systems. In the near term, these efforts may face significant challenges due to computational complexity, which could ultimately necessitate quantum computing resources. However, emerging machine learning technologies provide a promising avenue to tackle these complexities. For instance, deep learning strategies can be employed to extract insights from the vast datasets generated by joint experimental and theoretical efforts [137], enabling the prediction of molecular properties and their interactions with the environment. Beyond enhancing our understanding of microscopic dynamics, this line of research could also enable quantum control in molecular quantum technologies, opening new possibilities for engineering molecular systems with specific applications.

A second major challenge lies in the material domain. Host materials for single molecules, which so far has been almost exclusively limited to organic materials apart from a recent demonstration with hexagonal boron nitride (hBN) [138], often lack physical and chemical stability. Photostable single molecules are typically found in crystalline materials with long-range order. This is normally produced through sublimation in vacuum or inert gas atmosphere. Single molecules in polymeric hosts such as polyethylene [27] and polymethyl methacrylate [139] have also been reported, however, with sub-optimal photostability. Recently developed fabrication methods including liquid phase reprecipitation [90, 140] and electrohydrodynamic nanoprinting [89] could produce crystals with sizes in the micrometer to sub-micrometer scale, and enable Fourier-limited emission [141]. However, these hosts are fragile due to their low melting temperature, making them prone to sublimation. Additionally, their solubility in common organic solvents makes them hardly compatible with standard lithographic processing steps. To address this challenge, efforts in experiment and theory should be joined to identify an essential and adequate set of criteria to benchmark host-guest combinations. The search for physically and chemically stable, large bandgap host materials within the vast chemical space could benefit from integrating computational molecular screening techniques. High-throughput methods and machine learning-based approaches can efficiently predict the stability, electronic properties, and compatibility of potential host materials, enabling rapid identification of promising candidates [142]. The recent discovery of significant line narrowing of single molecules on the surface of hBN [138] opens a promising prospect to extend the chemical space of host materials beyond organics.

In addition to identifying new host materials, the deterministic integration of single molecules into nanoscale photonic and electronic devices is essential for achiev-

ing scalability in these technologies. A third challenge lies in the positioning of single molecules with the desired accuracy. Various approaches have been explored so far. For example, sparsely distributed nanocrystals could be identified through optical microscopy, and photonic structures can be fabricated directly around the selected molecule through direct laser writing [25]. Alternatively, sublimated flakes of the host material can be picked up using a fiber tip and transferred onto a desired location on a substrate using micro-manipulation [26]. Electrohydrodynamic nanoprinting has demonstrated the capability to place molecules on a substrate with lateral precision of approximately 100 nm [89]. Despite these advances, deterministic positioning of individual molecules with atomic-scale precision and assembly of multiple molecules into ordered arrays are still outstanding challenges. It is thus crucial to develop new methodologies for deterministically positioning molecules within the material. Notably, such deterministic positioning and ordering has been demonstrated in surface science experiments, for example, through tip manipulation in a scanning-tunneling microscope (STM) [143, 144]. However, the conditions of surface science experiments differ considerably with respect to those of quantum optics, from the required material substrate to vacuum conditions and to optical imaging techniques. Technical challenges need to be addressed to bridge the experimental settings of these two fields. Two-dimensional (2D) materials [138, 145] present a promising solution, potentially serving as substrates suitable for both STM manipulations and quantum optical measurements. For example, nanoscopic positioning and alignment of molecules on a 2D-material substrate can be performed on an STM. The substrate can be transferred for stacking of van-der-Waals heterostructures and fabrication of quantum devices.

## V. DISCUSSIONS AND CONCLUSION

So far, we have introduced the various degrees of freedom in the molecular guest-host system, elaborated on their interactions, and discussed their potential applications in advancing quantum technologies. Specifically, we focused on the vibrational and spin degrees of freedom, and examined the feasibility of constructing vibrational quantum memory, spin-photon interfaces, molecular spin registers, and investigation of molecular optomechanics.

In addition to these paths, it is worth noting that

the narrow ZPL of PAH molecules makes them highly sensitive probes of their local physical environment, such as electric fields and strain. Frequency tuning of the ZPL transition via the DC Stark effect has been routinely performed on single molecules. The demonstrated high electric field sensitivity of DBT molecules in 2,3-dibromonaphthalene matrix theoretically enables the detection of single electrons in the vicinity of the molecule [146]. This capability opens a wide range of possibilities for interfacing with quantum electronic devices, such as superconducting circuits [147], electron-based qubit devices in semiconductors [148, 149] and 2D materials [150]. Furthermore, it will also be worth investigating molecules with a permanent dipole moment for providing higher charge sensitivity [151]. In addition, the large strain susceptibilities of these molecules could also be utilized to interface with other quantum systems. For example, molecular spin degrees of freedom [152] could potentially benefit from such phononic couplings, to achieve couplings through a phononic bus [153]. Such phononic platforms could be realized with polymer host matrices feasible for nanostructuring, printing nanocrystals, or placing single molecules on conventional phononic structures [38, 89]. In a similar vein, pseudolocal vibrational modes could offer new ways to entangle molecules located at intermediate distances, bridging the electronic and phononic length scales and paving the way for the creation of collective many-body states.

Looking forward, single molecules as hybrid systems offer a range of potential quantum applications. They come with unique flexibility in host-guest combinations, allowing chemical tuning over the quantum mechanical properties of both the guest and the host. Despite challenges in theoretical understandings and fabrication techniques, we expect molecular host-guest systems to play a significant role in future solid-state quantum technologies.

## ACKNOWLEDGEMENT

We thank Michael Ruggenthaler for his valuable comments on the manuscript, and Leonardo dos Anjos Cunha for his help analyzing CCSD simulation results. D.W. acknowledges financial support from Germany's Excellence Strategy - Cluster of Excellence Matter and Light for Quantum Computing (ML4Q) EXC 2004/1-390534769 and the European Union (ERC, MSpin, 101077866).

- 
- [1] W. E. Moerner and L. Kador, Phys. Rev. Lett. **62**, 2535 (1989).
  - [2] M. Orrit and J. Bernard, Phys. Rev. Lett. **65**, 2716 (1990).
  - [3] C. Toninelli, I. Gerhardt, A. Clark, A. Reserbat-Plantey, S. Götzinger, Z. Ristanović, M. Colautti, P. Lombardi, K. Major, I. Deperasińska, *et al.*, Nat.

- Mater. , 1 (2021).
- [4] S. Adhikari and M. Orrit, J. Chem. Phys. **156**, 160903 (2022).
- [5] R. Lettow, Y. Rezus, A. Renn, G. Zumofen, E. Ikonen, S. Götzinger, and V. Sandoghdar, Phys. Rev. Lett. **104**, 123605 (2010).

- [6] M. Rezai, J. Wrachtrup, and I. Gerhardt, *Phys. Rev. X* **8**, 031026 (2018).
- [7] R. Duquennoy, M. Colautti, R. Emadi, P. Majumder, P. Lombardi, and C. Toninelli, *Optica* **9**, 731 (2022).
- [8] J. Hwang, M. Pototschnig, R. Lettow, G. Zumofen, A. Renn, S. Götzinger, and V. Sandoghdar, *Nature* **460**, 76 (2009).
- [9] A. Maser, B. Gmeiner, T. Utikal, S. Götzinger, and V. Sandoghdar, *Nat. Photonics* **10**, 450 (2016).
- [10] A. Pscherer, M. Meierhofer, D. Wang, H. Kelkar, D. Martín-Cano, T. Utikal, S. Götzinger, and V. Sandoghdar, *Phys. Rev. Lett.* **127**, 133603 (2021).
- [11] U. P. Wild, F. Güttler, M. Pirotta, and A. Renn, *Chem. Phys. Lett.* **193**, 451 (1992).
- [12] K. G. Schädler, C. Ciancico, S. Pazzagli, P. Lombardi, A. Bachtold, C. Toninelli, A. Reserbat-Plantey, and F. H. L. Koppens, *Nano Lett.* **19**, 3789 (2019).
- [13] M. Colautti, F. S. Piccioli, Z. Ristanović, P. Lombardi, A. Moradi, S. Adhikari, I. Deperasinska, B. Kozankiewicz, M. Orrit, and C. Toninelli, *ACS Nano* **14**, 13584 (2020).
- [14] M. Croci, H.-J. Müschenborn, F. Güttler, A. Renn, and U. P. Wild, *Chem. Phys. Lett.* **212**, 71 (1993).
- [15] Y. Tian, P. Navarro, and M. Orrit, *Phys. Rev. Lett.* **113**, 135505 (2014).
- [16] A. Fasoulakis, K. D. Major, R. A. Hoggarth, P. Burdakin, D. P. Bogusz, R. C. Schofield, and A. S. Clark, *Nanoscale* **15**, 177 (2023).
- [17] Y. L. A. Rezus, S. G. Walt, R. Lettow, A. Renn, G. Zumofen, S. Götzinger, and V. Sandoghdar, *Phys. Rev. Lett.* **108**, 093601 (2012).
- [18] D. Wang, H. Kelkar, D. Martín-Cano, D. Rattenbacher, A. Shkarin, T. Utikal, S. Götzinger, and V. Sandoghdar, *Nat. Phys.* **15**, 483 (2019).
- [19] K. G. Lee, X. W. Chen, H. Eghlidi, P. Kukura, R. Lettow, A. Renn, V. Sandoghdar, and S. Götzinger, *Nat. Photonics* **5**, 166 (2011).
- [20] X.-L. Chu, S. Götzinger, and V. Sandoghdar, *Nat. Photonics* **11**, 58 (2017).
- [21] J. Zirkelbach, B. Gmeiner, J. Renger, P. Türschmann, T. Utikal, S. Götzinger, and V. Sandoghdar, *Phys. Rev. Lett.* **125**, 103603 (2020).
- [22] S. Faez, P. Türschmann, H. R. Haakh, S. Götzinger, and V. Sandoghdar, *Phys. Rev. Lett.* **113**, 213601 (2014).
- [23] S. M. Skoff, D. Papencordt, H. Schauffert, B. C. Bayer, and A. Rauschenbeutel, *Phys. Rev. A* **97**, 043839 (2018).
- [24] S. Grandi, M. P. Nielsen, J. Cambiasso, S. Boissier, K. D. Major, C. Reardon, T. F. Krauss, R. F. Oulton, E. A. Hinds, and A. S. Clark, *APL Photonics* **4**, 086101 (2019).
- [25] M. Colautti, P. Lombardi, M. Trapuzzano, F. S. Piccioli, S. Pazzagli, B. Tiribilli, S. Nocentini, F. S. Cataliotti, D. S. Wiersma, and C. Toninelli, *Adv. Quantum Technol.* **3**, 2000004 (2020).
- [26] P. Ren, S. Wei, W. Liu, S. Lin, Z. Tian, T. Huang, J. Tang, Y. Shi, and X.-W. Chen, *Nat. Commun.* **13**, 3982 (2022).
- [27] D. Rattenbacher, A. Shkarin, J. Renger, T. Utikal, S. Götzinger, and V. Sandoghdar, *Optica* **10**, 1595 (2023).
- [28] C. Hettich, C. Schmitt, J. Zitzmann, S. Kühn, I. Gerhardt, and V. Sandoghdar, *Science* **298**, 385 (2002).
- [29] J.-B. Trebbia, Q. Deplano, P. Tamarat, and B. Lounis, *Nat. Commun.* **13**, 2962 (2022).
- [30] C. M. Lange, E. Daggett, V. Walther, L. Huang, and J. D. Hood, *Nat. Phys.* **1**, 1 (2024).
- [31] A. Shkarin, D. Rattenbacher, J. Renger, S. Hönl, T. Utikal, P. Seidler, S. Götzinger, and V. Sandoghdar, *Phys. Rev. Lett.* **126**, 133602 (2021).
- [32] V. Puller, B. Lounis, and F. Pistolesi, *Phys. Rev. Lett.* **110**, 125501 (2013).
- [33] P. Bunker, P. Jensen, N. R. C. Canada, and N. R. C. C. M. P. Program, *Molecular Symmetry and Spectroscopy*, NRC monograph publishing program (NRC Research Press, 2006).
- [34] C. M. Tesch and R. de Vivie-Riedle, *Phys. Rev. Lett.* **89**, 157901 (2002).
- [35] V. V. Albert, J. P. Covey, and J. Preskill, *Phys. Rev. X* **10**, 031050 (2020).
- [36] B. L. Augenbraun, L. Anderegg, C. Hallas, Z. D. Lasner, N. B. Vilas, and J. M. Doyle, Direct laser cooling of polyatomic molecules, in *Advances in Atomic, Molecular, and Optical Physics* (Elsevier, 2023) p. 89–182.
- [37] S. L. Bayliss, D. W. Laorenza, P. J. Mintun, B. D. Kovos, D. E. Freedman, and D. D. Awschalom, *Science* **370**, 1309 (2020).
- [38] B. Gurlek, V. Sandoghdar, and D. Martín-Cano, *Phys. Rev. Lett.* **127**, 123603 (2021).
- [39] A. Mena, S. K. Mann, A. Cowley-Semple, E. Bryan, S. Heutz, D. R. McCamey, M. Attwood, and S. L. Bayliss, *Phys. Rev. Lett.* **133**, 120801 (2024).
- [40] M. O. E. Steiner, J. S. Pedernales, and M. B. Plenio, Pentacene-doped naphthalene for levitated optomechanics (2024), arXiv:2405.13869 [quant-ph].
- [41] D. J. Diestler and A. H. Zewail, *J. Chem. Phys.* **71**, 3103 (1979).
- [42] B. Gurlek, *Turning an Organic Molecule into an Efficient Optomechanical System*, Doctoral dissertation, Friedrich-Alexander-Universität Erlangen-Nürnberg (FAU) (2023).
- [43] R. Smit, Z. Ristanovic, I. Deperasińska, B. Kozankiewicz, and M. Orrit, *ChemPhysChem* **25**, e202300881 (2024).
- [44] N. J. Turro, V. Ramamurthy, J. C. Scaiano, *et al.*, *Modern molecular photochemistry of organic molecules*, Vol. 188 (University Science Books Sausalito, CA, 2010).
- [45] K. Miyokawa and Y. Kurashige, *J. Phys. Chem. A* **128**, 2349 (2024), pMID: 38501814.
- [46] M. Reitz, C. Sommer, B. Gurlek, V. Sandoghdar, D. Martín-Cano, and C. Genes, *Phys. Rev. Res.* **2**, 033270 (2020).
- [47] I. Osad'ko, *Selective spectroscopy of single molecules* (Springer-Verlag, Heidelberg, 2013).
- [48] F.-F. Kong, X.-J. Tian, Y. Zhang, Y.-J. Yu, S.-H. Jing, Y. Zhang, G.-J. Tian, Y. Luo, J.-L. Yang, Z.-C. Dong, *et al.*, *Nat. Commun.* **12**, 1280 (2021).
- [49] R. Englman and J. Jortner, *Mol. Phys.* **18**, 145 (1970).
- [50] N. S. Bassler, M. Reitz, R. Holzinger, A. Vibók, G. J. Halász, B. Gurlek, and C. Genes, Generalized energy gap law: An open system dynamics approach to non-adiabatic phenomena in molecules (2024), arXiv:2405.08718.
- [51] C. Erker and T. Basché, *J. Am. Chem. Soc.* **144**, 14053 (2022).
- [52] G. P. Srivastava, *The physics of phonons* (Taylor & Francis Group, 1990).



- [53] M. Kasha, *Discuss. Faraday Soc.* **9**, 14 (1950).
- [54] J. L. Skinner, *Annu. Rev. Phys. Chem.* **39**, 463 (1988).
- [55] C. V. Raman and K. S. Krishnan, *Nature* **121**, 501 (1928).
- [56] G. Kresse and J. Hafner, *Phys. Rev. B* **47**, 558 (1993).
- [57] G. Kresse and J. Hafner, *Phys. Rev. B* **49**, 14251 (1994).
- [58] G. Kresse and J. Furthmüller, *Comput. Mater. Sci.* **6**, 15 (1996).
- [59] G. Kresse and J. Furthmüller, *Phys. Rev. B* **54**, 11169 (1996).
- [60] J. P. Perdew, K. Burke, and M. Ernzerhof, *Phys. Rev. Lett.* **77**, 3865 (1996).
- [61] A. Tkatchenko and M. Scheffler, *Phys. Rev. Lett.* **102**, 10.1103/PhysRevLett.102.073005. (2009).
- [62] A. Togo, *J. Phys. Soc. Jpn.* **92**, 012001 (2023).
- [63] P. Klemens, *Phys. Rev.* **148**, 845 (1966).
- [64] A. Nazir and D. P. McCutcheon, *J. Phys. Condens. Matter* **28**, 103002 (2016).
- [65] F. Zhang, M. Hayashi, H.-W. Wang, K. Tominaga, O. Kambara, J.-i. Nishizawa, and T. Sasaki, *J. Chem. Phys.* **140**, 174509 (2014).
- [66] D. D. Dlott, *Annu. Rev. Phys. Chem.* **37**, 157 (1986).
- [67] H. Fleischhauer, C. Krysch, B. Wagner, and H. Kupka, *J. Chem. Phys.* **97**, 1742 (1992).
- [68] S. Kummer, F. Kulzer, R. Kettner, T. Basché, C. Tietz, C. Glowatz, and C. Krysch, *J. Chem. Phys.* **107**, 7673 (1997).
- [69] J. Zirkelbach, M. Mirzaei, I. Deperasinska, B. Kozankiewicz, B. Gurlek, A. Shkarin, T. Utikal, S. Götzinger, and V. Sandoghdar, *J. Chem. Phys.* **156**, 104301 (2022).
- [70] S. Brueck and R. Osgood Jr, *Chem. Phys. Lett.* **39**, 568 (1976).
- [71] W. C. Campbell, G. C. Groenenboom, H.-I. Lu, E. Tsikata, and J. M. Doyle, *Phys. Rev. Lett.* **100**, 083003 (2008).
- [72] J. R. Hill, E. L. Chronister, T. C. Chang, H. Kim, J. C. Postlewaite, and D. D. Dlott, *J. Chem. Phys.* **88**, 2361 (1988).
- [73] G. Huang, A. Beccari, N. J. Engelsens, and T. J. Kippenberg, *Nature* **626**, 512 (2024).
- [74] J. Köhler, *Phys. Rep.* **310**, 261 (1999).
- [75] J. Köhler, A. Brouwer, E. J. Groenen, and J. Schmidt, *Science* **268**, 1457 (1995).
- [76] J. Wrachtrup, A. Gruber, L. Fleury, and C. Von Borczyskowski, *Chem. Phys. Lett.* **267**, 179 (1997).
- [77] F. Jelezko, T. Gaebel, I. Popa, M. Domhan, A. Gruber, and J. Wrachtrup, *Phys. Rev. Lett.* **93**, 130501 (2004).
- [78] T. J. Penfold, E. Gindensperger, C. Daniel, and C. M. Marian, *Chem. Rev.* **118**, 6975 (2018).
- [79] J. S. Wilson, N. Chawdhury, M. R. A. Al-Mandhary, M. Younus, M. S. Khan, P. R. Raithby, A. Köhler, and R. H. Friend, *J. Am. Chem. Soc.* **123**, 9412 (2001).
- [80] D. Beljonne, Z. Shuai, G. Pourtois, and J. L. Bredas, *The Journal of Physical Chemistry A* **105**, 3899 (2001).
- [81] A. B. Zahlan, *The triplet state* (Cambridge University Press, 1967).
- [82] J. Wrachtrup, C. Von Borczyskowski, J. Bernard, M. Orrit, and R. Brown, *Nature* **363**, 244 (1993).
- [83] J. Köhler, J. A. Disselhorst, M. Donckers, E. J. Groenen, J. Schmidt, and W. E. Moerner, *Nature* **363**, 242 (1993).
- [84] H. J. Kimble, *Nature* **453**, 1023 (2008).
- [85] L.-M. Duan, M. D. Lukin, J. I. Cirac, and P. Zoller, *Nature* **414**, 413 (2001).
- [86] M. K. Bhaskar, R. Riedinger, B. Machielse, D. S. Levonian, C. T. Nguyen, E. N. Knall, H. Park, D. Englund, M. Lončar, D. D. Sukachev, *et al.*, *Nature* **580**, 60 (2020).
- [87] K. Reim, J. Nunn, V. Lorenz, B. Sussman, K. Lee, N. Langford, D. Jaksch, and I. Walmsley, *Nat. Photonics* **4**, 218 (2010).
- [88] H. P. Specht, C. Nölleke, A. Reiserer, M. Uphoff, E. Figueroa, S. Ritter, and G. Rempe, *Nature* **473**, 190 (2011).
- [89] C. U. Hail, C. Höller, K. Matsuzaki, P. Rohner, J. Renger, V. Sandoghdar, D. Poulikakos, and H. Eghlidi, *Nat. Commun.* **10**, 1880 (2019).
- [90] S. Pazzagli, P. Lombardi, D. Martella, M. Colautti, B. Tiribilli, F. S. Cataliotti, and C. Toninelli, *ACS Nano* **12**, 4295 (2018).
- [91] S. Corcelli and J. Tully, *J. Chem. Phys.* **116**, 8079 (2002).
- [92] M. Aspelmeyer, T. J. Kippenberg, and F. Marquardt, *Rev. Mod. Phys.* **86**, 1391 (2014).
- [93] S. Barzanjeh, A. Xuereb, S. Gröblacher, M. Paternostro, C. A. Regal, and E. M. Weig, *Nat. Phys.* **18**, 15 (2022).
- [94] H. Ren, M. H. Matheny, G. S. MacCabe, J. Luo, H. Pfeifer, M. Mirhosseini, and O. Painter, *Nat. Commun.* **11**, 1 (2020).
- [95] A. Xomalis, X. Zheng, R. Chikkaraddy, Z. Koczor-Benda, E. Miele, E. Rosta, G. A. Vandenbosch, A. Martínez, and J. J. Baumberg, *Science* **374**, 1268 (2021).
- [96] M. Mirhosseini, A. Sipahigil, M. Kalaei, and O. Painter, *Nature* **588**, 599 (2020).
- [97] M. Atatüre, D. Englund, N. Vamivakas, S.-Y. Lee, and J. Wrachtrup, *Nat. Rev. Mater.* **3**, 38 (2018).
- [98] A. Reiserer, *Rev. Mod. Phys.* **94**, 041003 (2022).
- [99] D. Wang, *J. Phys. B* **54**, 133001 (2021).
- [100] K. Kim, A. Aepli, T. Bothwell, and J. Ye, *Phys. Rev. Lett.* **130**, 113203 (2023).
- [101] S. Truppe, S. Marx, S. Kray, M. Doppelbauer, S. Hofsäss, H. C. Schewe, N. Walter, J. Pérez-Ríos, B. G. Sartakov, and G. Meijer, *Phys. Rev. A* **100**, 052513 (2019).
- [102] N. Walter, J. Seifert, S. Truppe, H. C. Schewe, B. G. Sartakov, and G. Meijer, *J. Chem. Phys.* **156**, 184301 (2022).
- [103] J. M. Taylor, C. M. Marcus, and M. D. Lukin, *Phys. Rev. Lett.* **90**, 206803 (2003).
- [104] E. V. Denning, D. A. Gangloff, M. Atatüre, J. Mørk, and C. Le Gall, *Phys. Rev. Lett.* **123**, 140502 (2019).
- [105] Z. Kurucz, M. W. Sørensen, J. M. Taylor, M. D. Lukin, and M. Fleischhauer, *Phys. Rev. Lett.* **103**, 010502 (2009).
- [106] T. Eichhorn, M. Haag, B. van den Brandt, P. Hautle, and W. Wenckeback, *Chem. Phys. Lett.* **555**, 296 (2013).
- [107] Y. Quan, B. van den Brandt, J. Kohlbrecher, W. Wenckeback, and P. Hautle, *Nuclear Instruments and Methods in Physics Research Section A: Accelerators, Spectrometers, Detectors and Associated Equipment* **921**, 22 (2019).
- [108] A. C. J. Brouwer, J. Köhler, A. M. van Oijen, E. J. J. Groenen, and J. Schmidt, *J. Chem. Phys.* **110**, 9151 (1999).

- [109] A. Reiserer, N. Kalb, M. S. Blok, K. J. M. van Bemmel, T. H. Taminiau, R. Hanson, D. J. Twitchen, and M. Markham, *Phys. Rev. X* **6**, 021040 (2016).
- [110] A. Chiesa, S. Roca, S. Chicco, M. de Ory, A. Gómez-León, A. Gomez, D. Zueco, F. Luis, and S. Carretta, *Phys. Rev. Appl.* **19**, 064060 (2023).
- [111] A. Nowak-Król and F. Würthner, *Org. Chem. Front.* **6**, 1272 (2019).
- [112] S. Mais, J. Tittel, T. Basché, C. Bräuchle, W. Göhde, H. Fuchs, G. Müller, and K. Müllen, *J. Phys. Chem. A* **101**, 8435 (1997).
- [113] E. Lang, R. Hildner, H. Engelke, P. Osswald, F. Würthner, and J. Köhler, *ChemPhysChem* **8**, 1487 (2007).
- [114] D. D. Awschalom, R. Hanson, J. Wrachtrup, and B. B. Zhou, *Nat. Photonics* **12**, 516 (2018).
- [115] P. J. Linstrom and W. G. Mallard, *J. Chem. Eng. Data* **46**, 1059 (2001).
- [116] C. Lee, W. Yang, and R. G. Parr, *Phys. Rev. B* **37**, 785–789 (1988).
- [117] A. D. Becke, *J. Chem. Phys.* **98**, 1372–1377 (1993).
- [118] P. J. Stephens, F. J. Devlin, C. F. Chabalowski, and M. J. Frisch, *J. Phys. Chem.* **98**, 11623–11627 (1994).
- [119] F. Weigend and R. Ahlrichs, *Phys. Chem. Chem. Phys.* **7**, 3297 (2005).
- [120] A. Hellweg, C. Hättig, S. Höfener, and W. Klopper, *Theor. Chem. Acc.* **117**, 587–597 (2007).
- [121] S. Grimme, J. Antony, S. Ehrlich, and H. Krieg, *J. Chem. Phys.* **132**, 10.1063/1.3382344 (2010).
- [122] S. Grimme, S. Ehrlich, and L. Goerigk, *J. Comput. Chem.* **32**, 1456–1465 (2011).
- [123] R. Berraud-Pache, F. Neese, G. Bistoni, and R. Izsák, *J. Chem. Theory Comput.* **16**, 564 (2019).
- [124] Sanyam, R. Khatua, and A. Mondal, *J. Phys. Chem. A* 10.1021/acs.jpca.3c05056 (2023).
- [125] F. Neese, *Wiley Interdiscip. Rev. Comput. Mol. Sci.* **12**, e1606 (2022).
- [126] B. Sanchez-Lengeling and A. Aspuru-Guzik, *Science* **361**, 360 (2018).
- [127] J. Köhler, A.-J. C. Brouwer, E. J. J. Groenen, and J. Schmidt, *J. Am. Chem. Soc.* **120**, 1900 (1998).
- [128] S. Adhikari, R. Smit, and M. Orrit, *J. Phys. Chem. C* **0**, null (0).
- [129] B. Gmeiner, A. Maser, T. Utikal, S. Götzinger, and V. Sandoghdar, *Phys. Chem. Chem. Phys.* **18**, 19588 (2016).
- [130] Z. Koczor-Benda, A. L. Boehmke, A. Xomalis, R. Arul, C. Readman, J. J. Baumberg, and E. Rosta, *Phys. Rev. X* **11**, 041035 (2021).
- [131] M. Abolhasani and E. Kumacheva, *Nat. Synth.* **2**, 483 (2023).
- [132] E. McRae, *J. Chem. Phys.* **61**, 562 (1957).
- [133] P. Bordat and R. Brown, *Chem. Phys. Lett* **291**, 153 (1998).
- [134] A. A. L. Nicolet, C. Hofmann, M. A. Kol’chenko, B. Kozankiewicz, and M. Orrit, *ChemPhysChem* **8**, 1215 (2007).
- [135] A. I. Bertoni, R. M. Fogarty, C. G. Sánchez, and A. P. Horsfield, *J. Chem. Phys.* **156**, 044110 (2022).
- [136] T. Basché, W. E. Moerner, M. Orrit, and U. P. Wild, *Single-Molecule Optical Detection, Imaging and Spectroscopy* (Verlag-Chemie, Munich, 1997).
- [137] V. Gebhart, R. Santagati, A. A. Gentile, E. M. Gauger, D. Craig, N. Ares, L. Banchi, F. Marquardt, L. Pezzè, and C. Bonato, *Nat. Rev. Phys.* 10.1038/s42254-022-00552-1 (2023).
- [138] R. Smit, A. Tebyani, J. Hameury, S. J. van der Molen, and M. Orrit, *Nat. Commun.* **14**, 7960 (2023).
- [139] A. Walser, G. Zumofen, A. Renn, S. Götzinger, and V. Sandoghdar, *Mol. Phys.* **107**, 1897 (2009).
- [140] R. C. Schofield, P. Burdekin, A. Fasoulakis, L. Devanz, D. P. Bogusz, R. A. Hoggarth, K. D. Major, and A. S. Clark, *ChemPhysChem* **23**, e202100809 (2022).
- [141] M. Musavinezhad, J. Renger, J. Zirkelbach, T. Utikal, C. U. Hail, T. Basché, D. Poulikakos, S. Götzinger, and V. Sandoghdar, *ACS Nano* **18**, 21886–21893 (2024).
- [142] A. M. Ferrenti, N. P. de Leon, J. D. Thompson, and R. J. Cava, *Npj Comput. Mater.* **6**, 10.1038/s41524-020-00391-7 (2020).
- [143] Y. Luo, G. Chen, Y. Zhang, L. Zhang, Y. Yu, F. Kong, X. Tian, Y. Zhang, C. Shan, Y. Luo, J. Yang, V. Sandoghdar, Z. Dong, and J. G. Hou, *Phys. Rev. Lett.* **122**, 233901 (2019).
- [144] L. Zhang, Y.-J. Yu, L.-G. Chen, Y. Luo, B. Yang, F.-F. Kong, G. Chen, Y. Zhang, Q. Zhang, Y. Luo, *et al.*, *Nat. Commun.* **8**, 580 (2017).
- [145] H. Wang, N. Stenger, P. Lyngby, M. Kuisma, and K. S. Thygesen, Two-dimensional materials as ideal substrates for molecular quantum emitters (2024), arXiv:2410.02292.
- [146] A. Moradi, Z. Ristanovic, M. Orrit, I. Deperasińska, and B. Kozankiewicz, *ChemPhysChem* **20**, 55 (2019).
- [147] S. Das, V. E. Elfving, S. Faez, and A. S. Sørensen, *Phys. Rev. Lett.* **118**, 140501 (2017).
- [148] V. Langrock, J. A. Krzywda, N. Focke, I. Seidler, L. R. Schreiber, and L. Cywiński, *PRX Quantum* **4**, 020305 (2023).
- [149] G. Burkard, T. D. Ladd, A. Pan, J. M. Nichol, and J. R. Petta, *Rev. Mod. Phys.* **95**, 025003 (2023).
- [150] K. Hecker, L. Banszerus, A. Schäpers, S. Möller, A. Peters, E. Icking, K. Watanabe, T. Taniguchi, C. Volk, and C. Stampfer, *Nat. Commun.* **14**, 7911 (2023).
- [151] S. Faez, N. R. Verhart, M. Markoulides, F. Buda, A. Gourdon, and M. Orrit, *Faraday Discuss.* **184**, 251 (2015).
- [152] D. W. Laorenza and D. E. Freedman, *J. Am. Chem. Soc.* **144**, 21810 (2022).
- [153] M. C. Kuzyk and H. Wang, *Phys. Rev. X* **8**, 041027 (2018).